



HHS Public Access

Author manuscript

Kidney Int. Author manuscript; available in PMC 2020 August 13.

Published in final edited form as:

Kidney Int. 2011 May ; 79(9): 957–965. doi:10.1038/ki.2010.534.

The canonical Wnt signaling pathway is not involved in renal cyst development in the kidneys of *inv* mutant mice

Noriyuki Sugiyama¹, Tadasuke Tsukiyama², Terry P. Yamaguchi³, Takahiko Yokoyama¹

¹Department of Anatomy and Developmental Biology, Graduate School of Medical Science, Kyoto Prefectural University of Medicine, Kyoto, Japan

²Department of Biochemistry, Hokkaido University Graduate School of Medicine, Hokkaido, Japan

³Cancer and Developmental Biology Laboratory, National Cancer Institute-National Institute of Health, Frederick, Maryland, USA

Abstract

Recent studies have identified several genes whose defects cause hereditary renal cystic diseases with most of the gene products located in the primary cilia. It has been suggested that primary cilia are involved in signaling pathways, defects of which result in abnormal cell proliferation and randomization of oriented cell division in the kidney leading to cyst formation. Mice with a mutation in the *inv* gene are a model for human nephronophthisis type 2 and develop multiple renal cysts. Inv protein (also called inversin) is located in the base of primary cilia and acts as a switch from canonical to non-canonical Wnt signaling. Here, we studied the orientation of cell division and proliferation in the kidneys of *inv* mutant mice, as its loss is thought to maintain activation of the canonical Wnt signaling. To establish if canonical signaling was involved in this process, we mated *inv* mutant with *BATlacZ* mice to measure canonical Wnt activity. Based on these reporter mice, nuclear localization and phosphorylation of β -catenin, and responsiveness to Wnt ligands in *inv* mutant cells, we found that random oriented cell division is an initial event for renal tubule expansion and precedes cell proliferation. Thus, our results do not support the hypothesis that canonical Wnt signaling causes renal cyst development in these mice.

The primary cilia are microtubule-based organelles that project from the surface of most vertebrate cells. Defects of cilia or ciliary proteins are known to cause many human diseases, collectively referred to as a ciliopathy, such as polycystic kidney disease (PKD), nephronophthisis, polydactyly, primary cilia dyskinesia, *situs inversus*, and Bardet–Biedl syndrome. Recent studies have suggested that primary cilia are involved in signaling pathways.¹ Defects of cilia and ciliary proteins are thought to affect these signaling pathways as well as its motility, which leads to various phenotypes.

Renal cysts are the most commonly observed phenotype among the ciliopathies. Although the mechanism by which ciliary defects cause cystic changes in the kidney are unknown,

Correspondence: Takahiko Yokoyama, Department of Anatomy and Developmental Biology, Kyoto Prefectural University of Medicine, Kawaramachi-Hirokoji, Kamigyo-ku, Kyoto 602-8566, Japan. tyoko@koto.kpu-m.ac.jp.

DISCLOSURE

All the authors declared no competing interests.

two common abnormalities, cell proliferation² and random oriented cell division,³ have been observed in almost all renal cystic diseases. In addition, as inhibition of cell proliferation suppresses cyst progression, cell proliferation is considered to be a key factor for progression of renal cysts.⁴ We and others have shown that extracellular signal-regulated protein kinase (ERK) signaling is activated in renal cysts, and suppression of ERK signaling inhibits renal cyst progression.^{5,6} Canonical Wnt signaling is another candidate signaling pathway for stimulation of renal cell proliferation. Activation of canonical Wnt signaling makes β -catenin interact with TCF/LEF family transcription factors and promotes specific gene expression to induce cell proliferation. Constitutive activation of *β -catenin* transgenic mice and *Apc*-null mice have been reported to cause severe polycystic kidney disease.^{7,8} Therefore, Wnt signaling is also a candidate intracellular pathway that may stimulate cell proliferation to cause cystic kidneys. Furthermore, a connection between canonical Wnt signaling and cilia has been reported.⁹ *Kif3*, *Ift88*, and *Odf1* are essential for ciliogenesis. Enhanced *β -catenin* transcriptional activation also has been reported in *kif3a* mutant embryos, and Wnt hyper-responsiveness has been observed in *kif3*, *ift88*, and *odf1* embryonic fibroblast cells.⁹ Target knockout of *kif3* in the kidney results in defective ciliogenesis and development of cystic kidneys, and abnormal β -catenin level and nuclear localization of β -catenin have been reported in *Kif3a*-deficient tubular epithelial cells.¹⁰ These results suggest that cilia have a function in restraining canonical Wnt signaling, and render the latter an attractive candidate signaling pathway for promotion of renal cell proliferation in cystic kidneys.

During proliferation of tubular epithelial cells, the dividing cells align along the longitudinal axis of the growing nephron. In some renal cystic mutants, this alignment is lost and cell division is oriented randomly.^{3,11–13} This random oriented cell division is the other possibility that induces cystic changes in the kidney. Two recent studies have suggested a relationship between oriented cell division in renal tubules and non-canonical Wnt signaling.^{12,13} *Fat4*, whose mutation leads to cystic kidney disease, genetically interacts with planar cell polarity genes *Vangl2* and *Fjx1*. *Fat4* mutant mice show that the angle of renal cell division is randomized. Defects in Wnt-9b signaling also randomize the angle of renal epithelial cell division and result in renal cyst formation. Thus, oriented cell division is considered to be managed by non-canonical Wnt/planar cell polarity signaling.

The *inv* gene has been identified as a causative gene for *inv* mutant mice that show reversal of left–right asymmetry, jaundice, and multiple renal cysts.¹⁴ The human *INVS* gene has been found to be responsible for nephronophthisis type 2.¹⁵ *Inv* protein acts as an intraciliary anchor for nephrocystin-3 and Nek8.^{16,17} It has been reported that *Inv* protein is required for conversion–extension movements during *Xenopus* gastrulation, and knockdown of *inv* in zebrafish causes pronephric cysts.¹⁸ Simons *et al.*¹⁸ have proposed that *Inv* inhibits canonical Wnt signaling by targeting cytoplasmic disheveled (*Dvl*) for degradation, and that loss of *Inv* protein leads to sustained activation of canonical Wnt signaling.¹⁸ This is an attractive hypothesis because it can explain both cell proliferation and random oriented cell division in renal cysts at the same time. However, these experiments were performed using *in vitro* and zebrafish systems. As far as we are aware, no investigation of Wnt signaling in *inv* mutant kidneys *in situ* has been carried out.

In this study, we examined renal cell proliferation and orientation of the mitotic spindle in *inv* kidney, and involvement of canonical Wnt signaling. We mated *BATlacZ* mice with *inv* mutant mice to investigate whether *inv* kidneys showed anomalous or enhanced lacZ expression. We also examined phosphorylation and localization of β -catenin in control and *inv* kidneys. We showed that random oriented cell division precedes cell proliferation, and that canonical Wnt signaling is not activated in *inv* kidneys.

RESULTS

Renal cell proliferation in control and *inv/inv* mice

To establish when *inv/inv* kidneys begin to show increased cell proliferation, we examined 16.5 dpc, newborn, and 5-day-old control and *inv/inv* kidneys. Kidneys of newborn and 5-day-old *inv/inv* mice showed higher expression of proliferating cell nuclear antigen and phospho-Rb than did age-matched controls, whereas no difference was observed in 16.5 dpc kidneys between control and *inv/inv* mice. Suppression of p21^{waf1/cip1} was observed only in 5-day-old *inv/inv* kidneys when compared with controls (Figure 1a).

At 16.5 dpc, percentages of renal tubules with > 50 μm in diameter in normal and *inv/inv* kidneys were 3.4 and 3.2%, respectively, and not significantly different (Figure 1b). As previously reported, renal tubules in diameter decrease from embryo to newborn.¹³ Almost all renal tubules in normal kidney after newborn were < 50 μm in diameter. In contrast, the percentage of renal tubules > 50 μm in diameter was 62.7% in newborn and 87.1% in 5-day-old *inv/inv* kidneys (Figure 1b). To establish a relationship between tubular diameter and number of proliferating cells, we carried out bromodeoxyuridine (BrdU) incorporation and analyzed the results depending on tubular size. BrdU incorporated cells in renal tubules < 50 μm in diameter did not differ significantly between control and *inv/inv* kidneys at newborn and 5-day-old (Figure 1c). However, BrdU incorporation in renal tubules > 50 μm in diameter in newborn and 5-day-old *inv/inv* kidneys was significantly increased when compared with incorporation in tubules < 50 μm in age-matched *inv/inv* and control kidneys. These results suggested that renal tubules > 50 μm in diameter contained more proliferating cells and were likely more responsible for high expression of cell cycle regulators. As there was no difference in the percentage of BrdU incorporated cells in tubules < 50 μm in diameter between *inv/inv* and control kidneys in newborn and 5-day-old mice, we defined renal tubules < 50 μm in diameter as normal or pre-cystic tubules.

Random oriented mitotic spindle in *inv/inv* kidneys

We next examined whether the loss of *inv* gene produced abnormalities in oriented cell division. Mitotic spindle has been reported to be oriented preferentially along the longitudinal axis of the growing nephron (Figure 2a left). However, orientation of mitotic spindles in *inv/inv* kidney was random to the longitudinal axis (Figure 2a right). We measured the orientation of mitotic spindles in pre-cystic tubules in neonatal *inv/inv* mice using the methods described by Fischer *et al.*³ and Patel *et al.*¹¹ We selected tubules < 50 μm in diameter from newborn control and *inv/inv* kidneys. Figure 2b shows all examined cell division angles that were illustrated with a line between 0 and 90 in quarter circles. Figure 2c summarizes percentages of tubules at intervals of 10 degrees about cell division angles. In

the control kidneys, 79.6% of the mitotic spindles were oriented within 40° along the longitudinal axis of the growing nephron (Figure 2b, left and 2c, open bars). In contrast, *inv/inv* kidneys indicated that this oriented alignment was lost and cell division was oriented randomly by the Kolmogorov–Smirnov test (Figure 2b, right and 2c, black bars).

Canonical Wnt/ β -catenin activity in control and *inv/inv* mutant kidneys

A previous study has suggested that *inv* inhibits canonical Wnt signaling and that lack of Inv protein leads to sustained activation of canonical Wnt signaling,¹⁸ which has been proposed to induce cell proliferation. Therefore, we examined canonical Wnt activity in *inv/inv* kidneys. The *inv/inv* mice were mated with *BATlacZ* mice that carried the *BATlacZ* gene. Canonical Wnt activity was assayed by monitoring the expression of the *BATlacZ* transgene, which has an *in vivo* reporter of Tcf/LEF function.¹⁹ The expression of the *BATlacZ* transgene was visualized by X-gal (5-bromo-4-chloro-3-indolyl- β -D-galactoside) staining. There was no significant difference between external appearance of X-gal staining of the control and *inv/inv* kidneys at all stages (Figure 3a). In control, reporter activity was downregulated specifically in the postnatal kidney, with residual activity only detectable in the cortex region (Figure 3b). Histological sections showed that the X-gal staining was seen in the ureteric bud tips and distal S-shaped body in newborn kidneys, and in the nephrogenic zone in postnatal control (+ / +) kidneys, and disappeared as nephrogenesis came to an end (Figure 3b). Further, medullar region in control kidneys showed very little X-gal staining. *Inv/inv* kidneys showed exactly the same signaling pattern as the control kidneys, and we did not observe any X-gal-positive expanded tubules. To quantify the *BATlacZ* reporter signals in the control and *inv/inv* kidneys, we performed enzyme-linked immunosorbent assay (ELISA) to detect transgene-specific β -galactosidase levels in kidneys at 16.5 dpc, newborn, and 5-day-old control and *inv/inv* mice (Figure 3c). The β -galactosidase level was decreased during the progress of kidney development, and there was no significant difference between control and *inv/inv* kidneys. These results showed that loss of the *inv* gene did not influence *BATlacZ* expression.

We also examined *inv C* mouse kidneys (*inv/inv, inv C::GFP*) carrying the *BATlacZ* transgene. *Inv C* mice start to develop renal cysts about 1 week after birth. *Inv C* kidneys had few X-gal signals, as did the controls (Figure 3c). Renal epithelial cells in *inv C* cystic kidneys were negative for X-gal staining.

In addition, no difference was observed in X-gal staining pattern and β -galactosidase level by ELISA during embryonic development at the left–right axis determination stage (Supplementary Figure S1 online).

Phosphorylation and localization of β -catenin and GSK3 β in control and *inv/inv* mutant cells

Next, we examined β -catenin localization using immunohistochemistry in 5-day-old control and *inv/inv* kidneys. β -Catenin was observed at the cell boundary and in the cytoplasm. However, we did not observe nuclear staining in either 5-day-old control or *inv/inv* kidneys (Figure 4a). Although some staining at the apical surface of tubular cells in *inv/inv* mice was observed, this did not differ significantly between control and *inv/inv* kidneys.

We also examined β -catenin accumulation in the nuclear and cytoplasmic fractions. Nuclear and cytoplasmic fractions were separated from 5-day-old control and *inv/inv* kidneys and collected. LiCl treatment of COS7 cells is known to increase nuclear translocation of β -catenin and these cells were used as controls.²⁰ The intensity of β -catenin signals in the nuclear fraction in *inv/inv* and control kidneys was almost identical (Figure 4b). No significant differences were observed between *inv/inv* and control kidneys when β -catenin signaling was compared with the corresponding histone H2B signal. β -Catenin at Ser33, 37, and Thr41 is phosphorylated by glycogen synthase kinase 3 β (GSK3 β) and canonical Wnt/ β -catenin signal is inactivated by degradation of phospho- β -catenin. We used a phospho- β -catenin antibody that recognized phosphorylation at all site.²¹ In cytoplasmic fractions, there was no significant difference in the signal intensity of β -catenin and phospho- β -catenin between *inv/inv* and control kidneys. E-cadherin and histone H2B were used as markers for cytoplasmic and nuclear fractions, respectively. No detectable contamination between these two fractions was observed.

Activation of ERK signaling in newborn *inv/inv* kidneys

We previously have shown that ERK is activated in kidneys of *inv* C mice, and that suppression of ERK activity inhibits renal cell proliferation in *invDC* mice.⁶ Therefore, we examined activation of ERK signaling in *inv/inv* kidneys. Total amount of ERK did not significantly differ between *inv/inv* and control kidneys in 16.5 dpc, newborn, and 5-day-old mice (Figure 5a). However, phospho-ERK was elevated significantly in *inv/inv* kidneys in both newborn and 5-day-old mice, but not 16.5 dpc embryos when compared with age-matched controls (Figure 5a and b). Immunohistochemistry confirmed that the phospho-ERK-positive cells were detected in the renal epithelial cells of *inv/inv* cystic kidneys (Figure 5c).

We also examined AKT and signal transducer and activator of transcription (STAT) signaling. STAT3 was activated in 5-day-old *inv/inv* kidneys, but AKT, STAT1, and STAT6 were not activated in *inv/inv* kidney (Supplementary Figure S2 online).

DISCUSSION

Random oriented cell division precedes cell proliferation

BrdU incorporation analysis suggested that tubules > 50 μ m in diameter contained a higher percentage of proliferating cells. BrdU incorporation in tubules < 50 μ m in diameter in newborn and 5-day-old kidneys was indistinguishable to that in tubules in non-cystic control mice. In addition, the diameter of almost all tubules in non-cystic control mice was < 50 μ m in newborn and 5-day-old kidneys. The percentage of tubules < 50 μ m in diameter increased with age in *inv* mutant kidneys. Therefore, tubules < 50 μ m in diameter can be considered to be normal or pre-cystic tubules. Our BrdU incorporation results suggested that renal cell proliferation started at the same time or just after renal tubules start to expand.

To establish a relationship between cell proliferation and oriented cell division, we carefully selected tubules < 50 μ m in diameter to determine the angle of the mitotic spindle. Oriented division in renal epithelial cells is strictly controlled at the developmental stage.¹³ During

nephron development, renal tubules elongate. To achieve lengthening of renal tubules, renal epithelial cells proliferate without increase in tubular diameter. Oriented cell division is thought to control the elongation of tubular length without increasing tubular diameter. Our results showed that oriented cell division in tubules < 50 μm in diameter was lost and randomized in *inv/inv* mutant kidneys. As cell proliferation was observed in tubules > 50 μm in diameter, the results indicated that loss of oriented cell division preceded cell proliferation and tubular expansion. Our results suggest that the former is an initial process for renal tubular expansion in *inv/inv* mice.

It has been reported that the cell division angle is largely disoriented in several renal cystic mice,^{3,12,22} although *pkd1* kidney is controversial.²³ *Wnt-9b* mutants also have been reported to show random orientation of renal tubular cell division that leads to cystic kidney diseases.¹³ We did not observe any abnormal expression of *Wnt-9b* and other Wnt ligands in kidneys at 16.5 dpc and newborn (Supplementary Figure S3a online). Therefore, the random oriented cell division seen in *inv* kidneys is not likely to be related to Wnt expression.

Canonical Wnt signaling is not altered in *inv/inv* mutants

β -Catenin has a central role in regulating Wnt signaling.²⁴ When Wnt signals are present, GSK3 β activity is inhibited, and β -catenin dissociates from adenomatous polyposis coli protein and enters the nucleus. Without Wnt signaling, β -catenin is phosphorylated and degraded. Therefore, if canonical Wnt signaling is activated in *inv/inv* kidneys, it is expected that β -catenin is localized in the nucleus. Our results showed that β -catenin was present at the cell boundary and in the cytoplasm, but nuclear staining was not observed in either control or *inv/inv* kidneys. Western blotting for β -catenin accumulation also showed identical levels of nuclear β -catenin between control and *inv/inv* kidney concentrate. *BATlacZ* signals *in vivo* in *inv/inv* and control kidney were observed in a small number of cells in cortex. Under activation of canonical Wnt signaling, β -catenin is also dephosphorylated. There was no significant difference in the signal intensity of β -catenin and phospho- β -catenin in the cytoplasmic fraction between *inv/inv* and control kidneys. Furthermore, no significant difference was detected in GSK3 β , an upstream factor of β -catenin, between normal and *inv/inv* kidneys. These results indicated that activity of canonical Wnt signaling pathway in *inv/inv* cystic kidney was not significantly different from that in normal kidney. Responsiveness to Wnt ligands is not significantly different between control and *inv/inv* mutant cells (Supplementary Figure S3b online).

All our results showed that activity of canonical Wnt signaling in the *inv/inv* kidney is indistinguishable from that in non-cystic control kidneys. The previous study by Simon *et al.*¹⁸ proposed that *Inv* acts as a switch from canonical to non-canonical Wnt signaling, and that loss of *Inv* protein leads to cyst formation due to excessive Wnt signaling. They examined *Inv* function using zebrafish and *Xenopus* systems, but not mouse kidney *in situ*. The present study examined *Inv* function in mouse kidney. Zebrafish pronephric duct is equivalent of mouse pronephros. Renal cysts examined in *inv* mutant are derived from metanephros. Therefore, *Inv* could function differently between pronephros and metanephros.

Continuous activation of *inv* driving a CMV promoter did not affect renal development,² supporting the present results that *inv* does not inhibit canonical Wnt pathway during renal development. The present results suggest that *Inv* functions on non-canonical Wnt signaling without affecting canonical Wnt signaling in mouse metanephric kidney.

Abnormal activation of canonical Wnt signaling is observed in kidney of conditional *Kif3* knockout mutant mice^{9,10} and *Pkd2* knockout mice.²⁵ It is interesting to see if *Inv* has any role in activation of canonical Wnt signaling in conditional *Kif3a* and *Pkd2* knockout mutant or if other mechanisms activate canonical Wnt signaling.

ERK signaling pathway is early response cascade in *inv/inv* kidney

We have shown previously that ERK is activated in *inv C* mutant kidneys, and that suppression of ERK activity inhibits renal cyst enlargement. The present study confirmed that ERK activity was elevated in newborn mice when cell proliferation starts. *Pkd1* and *Pkd2* are causative genes for autosomal dominant PKD. It has been reported that mouse embryos that lack *pkd1* have defective STAT-1 phosphorylation and p21^{waf1} induction.²⁶ Suppression of p21^{waf1} expression was observed in 5-day-old kidneys, but not in newborn *inv/inv* kidneys. Overexpression of phosphoSTAT3 was detected at later stages in *inv/inv* cystic kidneys. Although these abnormalities may contribute to later stages of renal cell proliferation in *inv/inv* kidneys, these pathways are unlikely to be involved in the early stage of cell proliferation in *inv/inv* cyst development. In contrast, ERK signaling is already activated in newborn *inv/inv* kidneys. Thus, ERK signaling is most likely to stimulate cell proliferation in the early stage of renal cell proliferation in *inv/inv* mutants.

In conclusion, random oriented cell division precedes cell proliferation in *inv/inv* kidneys. The present results did not support the previously proposed switching theory in Wnt signaling by *Inv* protein. On the basis of our results, the continuous activation of canonical Wnt signaling is not likely to be involved in cell proliferation and oriented cell division of *inv/inv* kidneys. The connection between cell proliferation and random oriented cell division is still unknown. It remains to be seen if *Inv* protein regulates cell proliferation and oriented cell division by independent pathways, or if random oriented cell division induces continuous renal cell proliferation.

MATERIALS AND METHODS

Animals

The *inv/inv* and *inv C::GFP(inv C)* mice were maintained as described previously.² The *inv/inv* and *inv C* mice were hybridized with FVB background during the fifth generation or more. The *inv/inv* and *inv C* mice were mated with *BATlacZ* mice and the pups were used in X-gal staining and ELISA analysis. For genotyping of mice we used tail DNA (16.5 dpc, newborn, and 5-day-old) and yolk sac DNA (8.5 and 9.5 dpc). All mice strains were maintained in a pathogen-free state in an animal facility of Kyoto Prefectural University of Medicine, Japan. The experimental protocol was permitted by the Committee for Animal Research, Kyoto Prefectural University of Medicine.

BAT/lacZ transgene activity detection

BAT/lacZ transgene activity was detected by X-gal staining and ELISA. Embryos and dissected kidneys were washed in phosphatebuffered saline (PBS), fixed for 1h in 4% paraformaldehyde, 0.04% NP-40 was added, and incubated in X-gal staining solution (0.2mol/l sodium phosphate, pH 7.3, 1mmol/l MgCl₂, 10mM potassium ferricyanide, 10mmol/l potassium ferricyanide, and 0.4mg/ml X-gal) for 4–16h. The samples were post-fixed and frozen in 22-oxacalctriol compound. Frozen sections (10mm) were observed in an Olympus microscope IX70 equipped with a DP70 digital camera (Olympus, Tokyo, Japan). Changes in β -Gal transgene expression were quantitated using a β -Gal ELISA kit (Roche Applied Science, Penzberg, Germany), normalizing according to total protein.

Histological analysis

For morphological evaluation, mouse kidneys were fixed in 4% paraformaldehyde in PBS and embedded in paraffin wax. Sections (4 μ m thick) were stained with hematoxylin and eosin according to standard protocols. The diameter of the renal tubules was measured in hematoxylin- and eosin-stained sections. The diameter was measured as the distance between the major axis (from basal membrane) of each tubule. At least three kidneys were used for one experiment group, and at least 200 tubules were counted in each kidney. Cell proliferations were assayed by using BrdU incorporation, as previously described.² Immunohistochemistry methods for β -catenin and phospho-ERK are described in the Supplementary Methods.27–29

Western blot analysis

Kidney samples for western blot analysis were prepared from total kidneys, as described previously.² SDS-polyacrylamide gel electrophoresis and immunoblotting were carried out by standard procedures. The signals were visualized with the ECL-Plus detection system (GE Healthcare Bio-Sciences, Tokyo, Japan). Quantitation of the chemiluminescent signals was performed with a digital imaging system (VersaDoc; Bio-Rad, Berkeley, CA).

Measurement of orientation of cell division in renal epithelial cells

The orientation of cell division was measured according to Fischer *et al.*³ and Patel *et al.*¹¹ Kidney frozen sections (30 μ m thick) were fixed in 4% paraformaldehyde in PBS at room temperature for 20min and incubated with primary antibody (anti-Entactin/ Nidogen, anti-Histone H3pS10) in PBS, 4% bovine serum albumin, 0.1% Triton X-100 overnight at 4°C. Sections were rinsed several times in PBS, 0.1% Triton X-100, and incubated with secondary antibody (Alexa Fluor-488 and Alexa Fluor-555) in PBS, 4% bovine serum albumin, and 0.1% Triton X-100 at 4°C for 3h. Labeled tubules that contained anaphase nuclei were identified and a Z-stack was taken using the Olympus Fluoview FV1000. We collected images without deconvolution, with a z-step from 0.3 to 1 μ m on sections. Normally, a stack of 30–50 images, surrounding an area of mitosis, is sufficient to perform the measurements. This stack of images was reconstituted as a three-dimensional representation. The three-dimensional coordinates of the mitotic spindles and tubules were exported into an Excel spreadsheet, and the angle between the two axes was calculated using

the formula used by Patel *et al.*¹¹ A total of 103 cells in anaphase or telophase from 14 control and 28 *inv/inv* mutant kidneys (after the neonatal period) were analyzed.

Supplementary Material

Refer to Web version on PubMed Central for supplementary material.

ACKNOWLEDGMENTS

We thank Kunitada Shimotohno for the pTcf7wt-BP-Luc and pTcf7mut-BP-Luc reporter plasmids, and Shinji Takada for Wnt-3a and Wnt-5a-producing L cells and pGKWnt-3a and pGKWnt-5a plasmids. This work was supported by Grants-in-Aid for Young Scientists from the Ministry of Education, Science, and Culture (19790587 and 21790818) to NS.

REFERENCES

- Berbari NF, O'Connor AK, Haycraft CJ et al. The primary cilium as a complex signaling center. *Curr Biol* 2009; 19: R526–R535. [PubMed: 19602418]
- Sugiyama N, Yokoyama T. Sustained cell proliferation of renal epithelial cells in mice with *inv* mutation. *Genes Cells* 2006; 11: 1213–1224. [PubMed: 16999740]
- Fischer E, Legue E, Doyen A et al. Defective planar cell polarity in polycystic kidney disease. *Nat Genet* 2006; 38: 21–23. [PubMed: 16341222]
- Bukanov NO, Smith LA, Klinger KW et al. Long-lasting arrest of murine polycystic kidney disease with CDK inhibitor roscovitine. *Nature* 2006; 444: 949–952. [PubMed: 17122773]
- Omori S, Hida M, Fujita H et al. Extracellular signal-regulated kinase inhibition slows disease progression in mice with polycystic kidney disease. *J Am Soc Nephrol* 2006; 17: 1604–1614. [PubMed: 16641154]
- Okumura Y, Sugiyama N, Tanimura S et al. ERK regulates renal cell proliferation and renal cyst expansion in *inv* mutant mice. *Acta Histochem Cytochem* 2009; 42: 39–45. [PubMed: 19492026]
- Saadi-Kheddouci S, Berrebi D, Romagnolo B et al. Early development of polycystic kidney disease in transgenic mice expressing an activated mutant of the beta-catenin gene. *Oncogene* 2001; 20: 5972–5981. [PubMed: 11593404]
- Qian CN, Knol J, Igarashi P et al. Cystic renal neoplasia following conditional inactivation of APC in mouse renal tubular epithelium. *J Biol Chem* 2005; 280: 3938–3945. [PubMed: 15550389]
- Corbit KC, Shyer AE, Dowdle WE et al. Kif3a constrains beta-catenin-independent Wnt signalling through dual ciliary and non-ciliary mechanisms. *Nat Cell Biol* 2008; 10: 70–76. [PubMed: 18084282]
- Lin F, Hiesberger T, Cordes K et al. Kidney-specific inactivation of the KIF3A subunit of kinesin-II inhibits renal ciliogenesis and produces polycystic kidney disease. *Proc Natl Acad Sci USA* 2003; 100: 5286–5291. [PubMed: 12672950]
- Patel V, Li L, Cobo-Stark P et al. Acute kidney injury and aberrant planar cell polarity induce cyst formation in mice lacking renal cilia. *Hum Mol Genet* 2008; 17: 1578–1590. [PubMed: 18263895]
- Saburi S, Hester I, Fischer E et al. Loss of Fat4 disrupts PCP signaling and oriented cell division and leads to cystic kidney disease. *Nat Genet* 2008; 40: 1010–1015. [PubMed: 18604206]
- Karner CM, Chirumamilla R, Aoki S et al. Wnt9b signaling regulates planar cell polarity and kidney tubule morphogenesis. *Nat Genet* 2009; 41: 793–799. [PubMed: 19543268]
- Mochizuki T, Saijoh Y, Tsuchiya K et al. Cloning of *inv*, a gene that controls left/right asymmetry and kidney development. *Nature* 1998; 395: 177–181. [PubMed: 9744276]
- Otto EA, Schermer B, Obara T et al. Mutations in *INVS* encoding inversin cause nephronophthisis type 2, linking renal cystic disease to the function of primary cilia and left-right axis determination. *Nat Genet* 2003; 34: 413–420. [PubMed: 12872123]

16. Shiba D, Yamaoka Y, Hagiwara H et al. Localization of *Inv* in a distinctive intraciliary compartment requires the C-terminal ninein-homolog-containing region. *J Cell Sci* 2009; 122: 44–54. [PubMed: 19050042]
17. Shiba D, Manning D, Koga H et al. *Inv* acts as a molecular anchor for *Nphp3* and *Nek8* in the proximal segment of primary cilia. *Cytoskeleton* 2010; 67: 112–119. [PubMed: 20169535]
18. Simons M, Gloy J, Ganner A et al. *Inversin*, the gene product mutated in nephronophthisis type II, functions as a molecular switch between Wnt signaling pathways. *Nat Genet* 2005; 37: 537–543. [PubMed: 15852005]
19. Nakaya MA, Biris K, Tsukiyama T et al. *Wnt3a* links left-right determination with segmentation and anteroposterior axis elongation. *Development* 2005; 132: 5425–5436. [PubMed: 16291790]
20. Yamamoto H, Kishida S, Kishida M et al. Phosphorylation of axin, a Wnt signal negative regulator, by glycogen synthase kinase-3 β regulates its stability. *J Biol Chem* 1999; 274: 10681–10684. [PubMed: 10196136]
21. Chung GG, Provost E, Kielhorn EP et al. Tissue microarray analysis of beta-catenin in colorectal cancer shows nuclear phospho-beta-catenin is associated with a better prognosis. *Clin Cancer Res* 2001; 7: 4013–4020. [PubMed: 11751495]
22. Happe H, Leonhard WN, van der Wal A et al. Toxic tubular injury in kidneys from *Pkd1*-deletion mice accelerates cystogenesis accompanied by dysregulated planar cell polarity and canonical Wnt signaling pathways. *Hum Mol Genet* 2009; 18: 2532–2542. [PubMed: 19401297]
23. Nishio S, Tian X, Gallagher AR et al. Loss of oriented cell division does not initiate cyst formation. *J Am Soc Nephrol* 2009; 21: 295–302. [PubMed: 19959710]
24. Logan CY, Nusse R. The Wnt signaling pathway in development and disease. *Annu Rev Cell Dev Biol* 2004; 20: 781–810. [PubMed: 15473860]
25. Kim I, Ding T, Fu Y et al. Conditional mutation of *Pkd2* causes cystogenesis and upregulates beta-catenin. *J Am Soc Nephrol* 2009; 20: 2556–2569. [PubMed: 19939939]
26. Bhunia AK, Piontek K, Boletta A et al. *PKD1* induces p21(waf1) and regulation of the cell cycle via direct activation of the JAK-STAT signaling pathway in a process requiring *PKD2*. *Cell* 2002; 109: 157–168. [PubMed: 12007403]
27. Shiba D, Takamatsu T, Yokoyama T. Primary cilia of *inv/inv* mouse renal epithelial cells sense physiological fluid flow: bending of primary cilia and Ca²⁺ influx. *Cell Struct Funct* 2005; 30: 93–100. [PubMed: 16474191]
28. Shibamoto S, Higano K, Takada R et al. Cytoskeletal reorganization by soluble Wnt-3a protein signalling. *Genes Cells* 1998; 3: 659–670. [PubMed: 9893023]
29. Ueda Y, Hijikata M, Takagi S et al. p73 β , a variant of p73, enhances Wnt/beta-catenin signaling in Saos-2 cells. *Biochem Biophys Res Commun* 2001; 283: 327–333. [PubMed: 11327702]

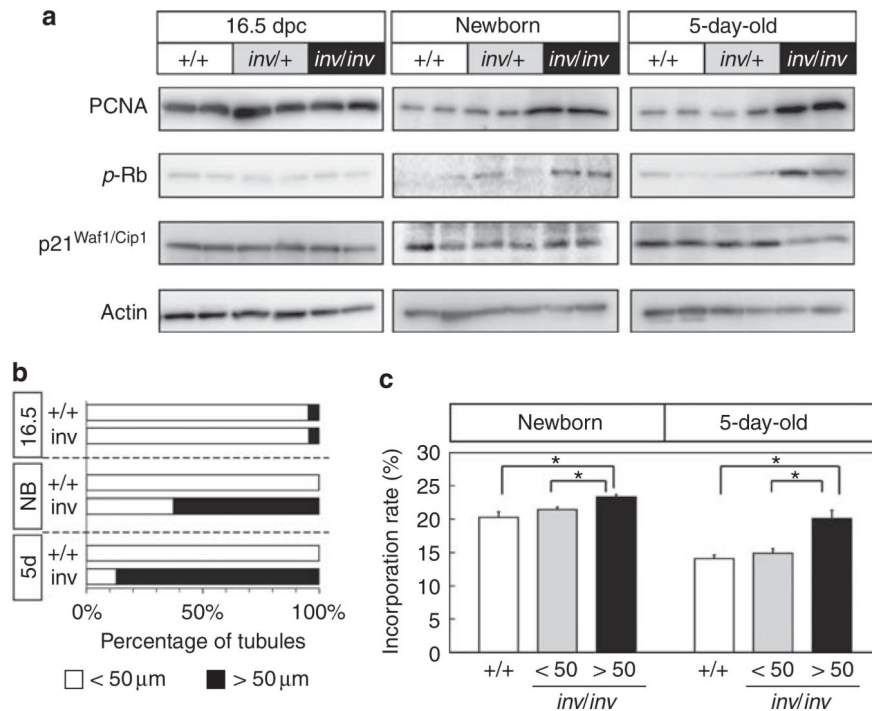


Figure 1 | Cell proliferation in control and *inv/inv* mutant kidneys.

(a) Immunoblot analysis of proliferating cell nuclear antigen (PCNA), *p-Rb*, and *p21^{Waf1/Cip1}* expression in 16.5 dpc, newborn, and 5-day-old control (+ / + and *inv* / +) and *inv/inv* mouse kidneys. Signal intensity of PCNA, *p-Rb*, and *p21^{Waf1/Cip1}* was compared with that of corresponding actin expression. (b) Percentage of < 50 μm (open bars) and > 50 μm (black bars) renal tubules in 16.5 dpc, newborn, and 5-day-old wild-type and *inv/inv* mice. (c) Percentage of bromodeoxyuridine (BrdU)-incorporated cells per number of renal epithelial cells examined in 5-day-old kidneys. At least 200 tubules in each of three kidneys were examined. Each bar represents the mean ± s.e. *Significantly different from controls using Student's *t*-test, with $P < 0.05$.

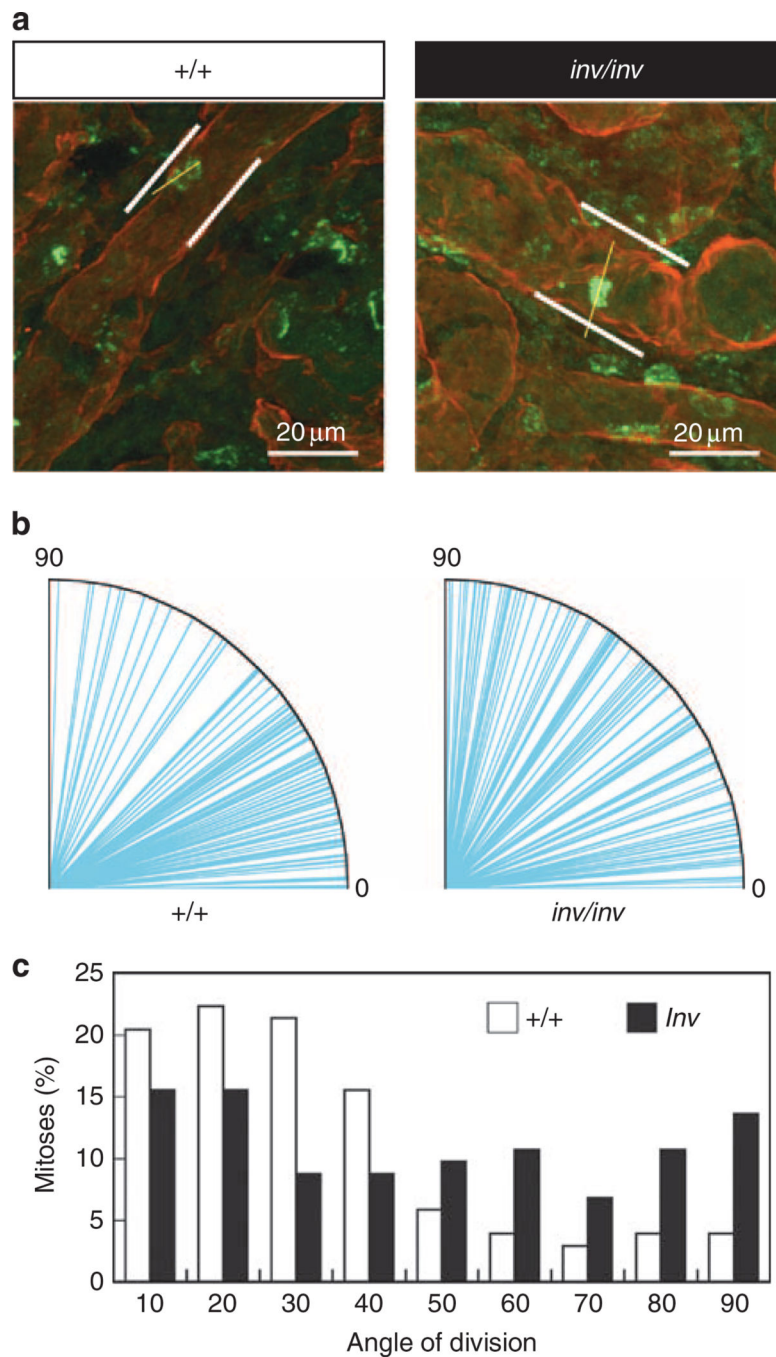


Figure 2 | Loss of *Inv* protein leads to random angle of cell division.

(a) Representative image of *inv/inv* mutant dividing cell. The axis of nephron is shown with two parallel white lines, and the orientation of mitotic spindle is shown with a yellow line. Basal membranes were stained with anti-Entactin antibody/Alexa 555, and dividing nuclei were stained with phospho-Histone H3 (ser10)/Alexa 488. (b) Quantification of cell division orientation in control (+ / +, left) and *inv/inv* mutant (right) mice. Each blue line indicated the angle of the mitotic spindles against the longitudinal axis of renal tubules. Angles for *inv/inv* mutants were random, whereas those of the controls were inclined forward

horizontally. (c) Graphical representation of the angle between the mitotic spindles and the longitudinal axis of renal tubules in newborn control (white bar) and *inv/inv* mutant (black bar) mice.

Author Manuscript

Author Manuscript

Author Manuscript

Author Manuscript

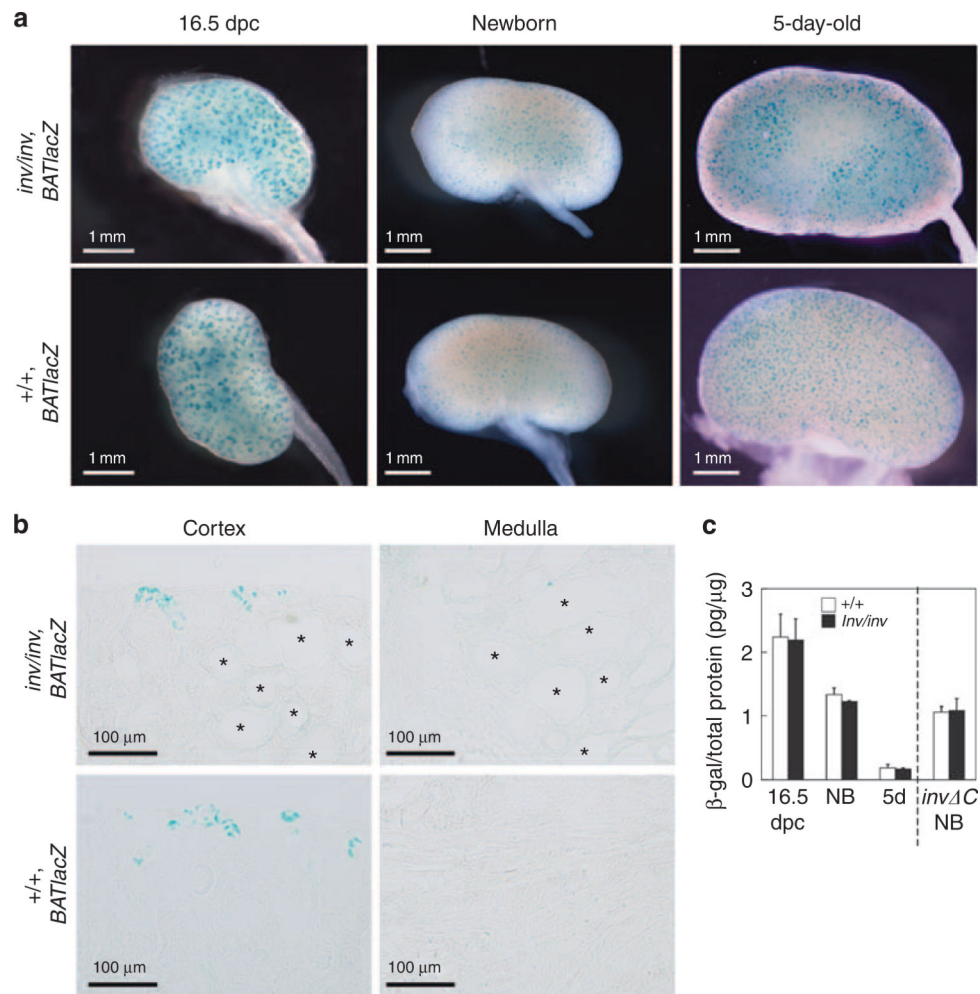


Figure 3 | X-gal (5-bromo-4-chloro-3-indolyl- β -D-galactoside) staining of kidneys of control and *inv/inv* mice carrying the *BATlacZ* reporter transgene.

(a) External appearance of X-gal staining of representative kidneys from control (+/+ , *BATlacZ*; lower) and *inv* (*inv/inv*, *BATlacZ*; upper) mice from 16.5 dpc through to 5 days of age. (b) The X-gal-positive staining of cortex and medulla in newborn control (lower) and *inv* (upper) kidneys. *cyst. (c) Quantitative analysis of *BATlacZ* reporter expression in *inv* and control kidney extracts. Transgene-specific β -galactosidase level was quantified by enzyme-linked immunosorbent assay. Control and *inv* kidneys all showed a similar level of *BATlacZ* expression. Each experimental group included at least three kidneys. 5d, 5-day-old; NB, newborn.

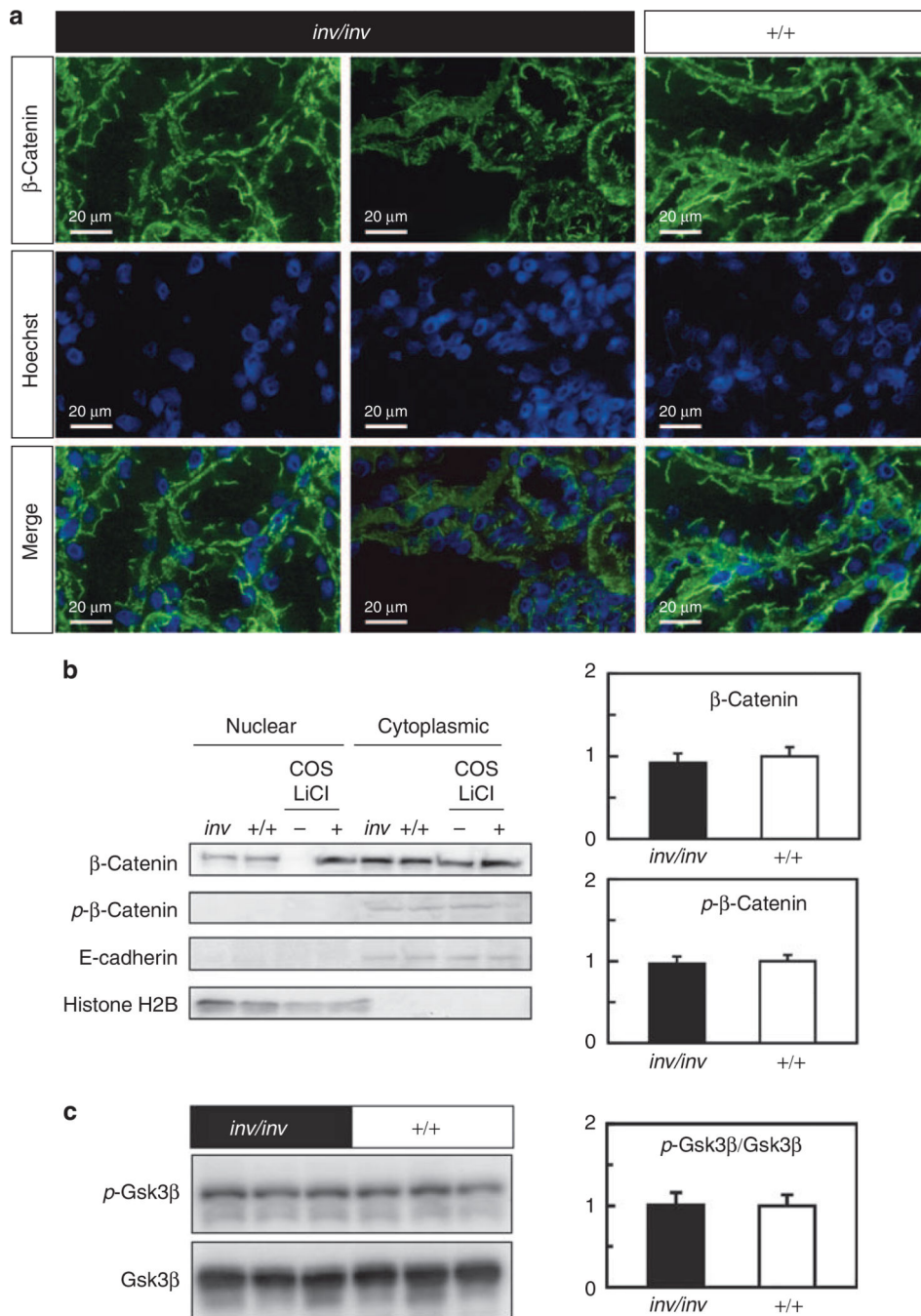


Figure 4 |. Canonical Wnt signaling was not activated in *inv* kidneys.

(a) Immunohistochemical localization of β -catenin (upper and lower, green) in 5-day-old *inv/inv* mutant and control (+ / +) kidneys. Signals for β -catenin were detected at the cell boundary and in the cytoplasm, but not in the nucleus. Counterstaining for the nucleus was performed with the chromosomal dye Hoechst 33342 (middle and lower, blue). Six kidneys from control and *inv/inv* mice were cut into 100 μ m sections, and examined. (b) Immunoblot analysis of β -catenin and phospho- β -catenin in nuclear and cytoplasmic fractions from the kidneys of 5-day-old control and *inv/inv* mutant mice. Densitometry results are shown in the

right panels. Ratios were determined as follows. Signal intensity of β -catenin and phospho- β -catenin was compared with that of histone H2B and β -catenin, respectively. The obtained values were further compared with the mean values from control kidneys. Data are the means \pm s.e. (relative to control) of four independent experiments. (c) Immunoblot analysis of glycogen synthase kinase 3 β (Gsk3 β) and phospho-Gsk3 β in kidneys of 5-day-old control and *inv/inv* mutant mice. Densitometry of total and phospho-Gsk3 β protein expression. Right panel indicated phospho-Gsk3 β expression relative to the corresponding total Gsk3 β protein expression. Ratios were determined as follows. Signal intensity of phospho-Gsk3 β was compared with that of the corresponding total Gsk3 β proteins. The obtained values were further compared with the mean values from + / + kidneys. Means \pm s.e. are shown.

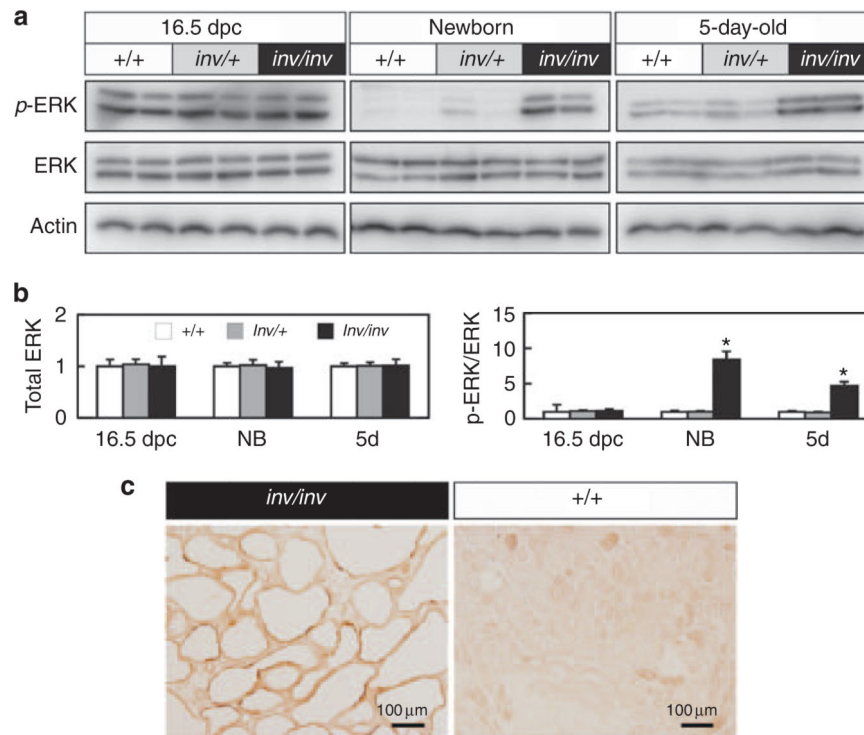


Figure 5 | Extracellular signal-regulated protein kinase (ERK) signaling in 16.5dpc, newborn, and 5-day-old control (+/+ and *inv/+*) and *inv/inv* kidneys.

(a) Western blots of phospho-ERK and total ERK protein in wild-type (+/+), *inv/+*, and *inv/inv* kidneys. Note that phospho-ERK was elevated in newborn (NB) and 5-day-old *inv/inv* mice. (b) Densitometry of total and phospho-ERK protein expression. Left panel indicated total ERK expression in 16.5 dpc, newborn, and 5-day-old mouse kidneys. Ratios were determined as follows. Signal intensity of total ERK was compared with that of the corresponding actin protein. The obtained values were further compared with the mean value from +/+ kidneys. Control (+/+) ($n = 8$), *inv/+* mice ($n = 8$), and the *inv/inv* mice ($n = 8$) were examined. Right panel indicated phospho-ERK expression relative to the corresponding total ERK protein expression. Ratios were determined as follows. Signal intensity of phospho-ERK was compared with that of the corresponding total ERK proteins. The obtained values were further compared with the mean values from +/+ kidneys. Means \pm s.e. are shown. *Significantly different from +/+ mice of the same age using Student's t -test, with $P < 0.01$. (c) Localization of phospho-ERK protein in renal epithelial cells. Phospho-ERK was detected in renal epithelial cells of both 5-day-old *inv/inv* mutant (left) and wild-type (+/+) (right) mouse kidneys.